Measurements of Low Temperature Dielectronic Recombination in L-Shell Iron for Modeling X-Ray Photoionized Cosmic Plasmas

D. W. Savin*, N. R. Badnell†, T. Bartsch‡, E. Behar*, C. Brandau‡, M. H. Chen‖, M. Grieser¶, T. W. Gorczyca§, G. Gwinner¶, A. Hoffknecht‡, S. M. Kahn*, A. Müller‡, R. Repnow¶, A. A. Saghiri¶, S. Schippers‡, M. Schmitt¶, D. Schwalm¶, A. Wolf¶, and P. A. Závodszky**

*Columbia Astrophysics Laboratory, Columbia University, New York, NY 10027, USA
†Department of Physics and Applied Physics, University of Strathclyde, Glasgow, G4 0NG, United Kingdom
‡Institut für Kernphysik, Justus-Liebig-Universität, D-35392 Giessen, Germany
‖Lawrence Livermore National Laboratory, Livermore, CA 94550, USA
¶Max-Planck-Institut für Kernphysik, D-69117 Heidelberg, Germany
§Department of Physics, Western Michigan University, Kalamazoo, MI, 49008, USA
**National Superconducting Cyclotron Laboratory, Michigan State University, East Lansing, MI, 48824 USA

Abstract. The iron L-shell ions (Fe^{17+} to Fe^{23+}) play an important role in determining the thermal and ionization structures and line emission from photoionized plasmas. Current uncertainties in the theoretical low temperature dielectronic recombination (DR) rate coefficients for these ions significantly affect our ability to model and interpret the line emission from observations of photoionized plasmas. To help resolve this issue, we have initiated a program of laboratory measurements to produce reliable low temperature DR rates for the L-shell iron. Here we present some of our recent results and discuss some of the astrophysical implications.

INTRODUCTION

X-ray photoionized plasmas are predicted [1] to form in the media surrounding accretion-powered compact sources such as X-ray binaries (XRBs) [2] and active galactic nuclei (AGN) [3]. In these plasmas, at low densities, the ionization structure depends on the shape of the ionizing spectrum, the metallicity of the gas, additional heating and/or cooling mechanisms, and radiative transfer effects. In

CP547, *Atomic Processes in Plasmas: Twelfth Topical Conf.*, edited by R. C. Mancini and R. A. Phaneuf

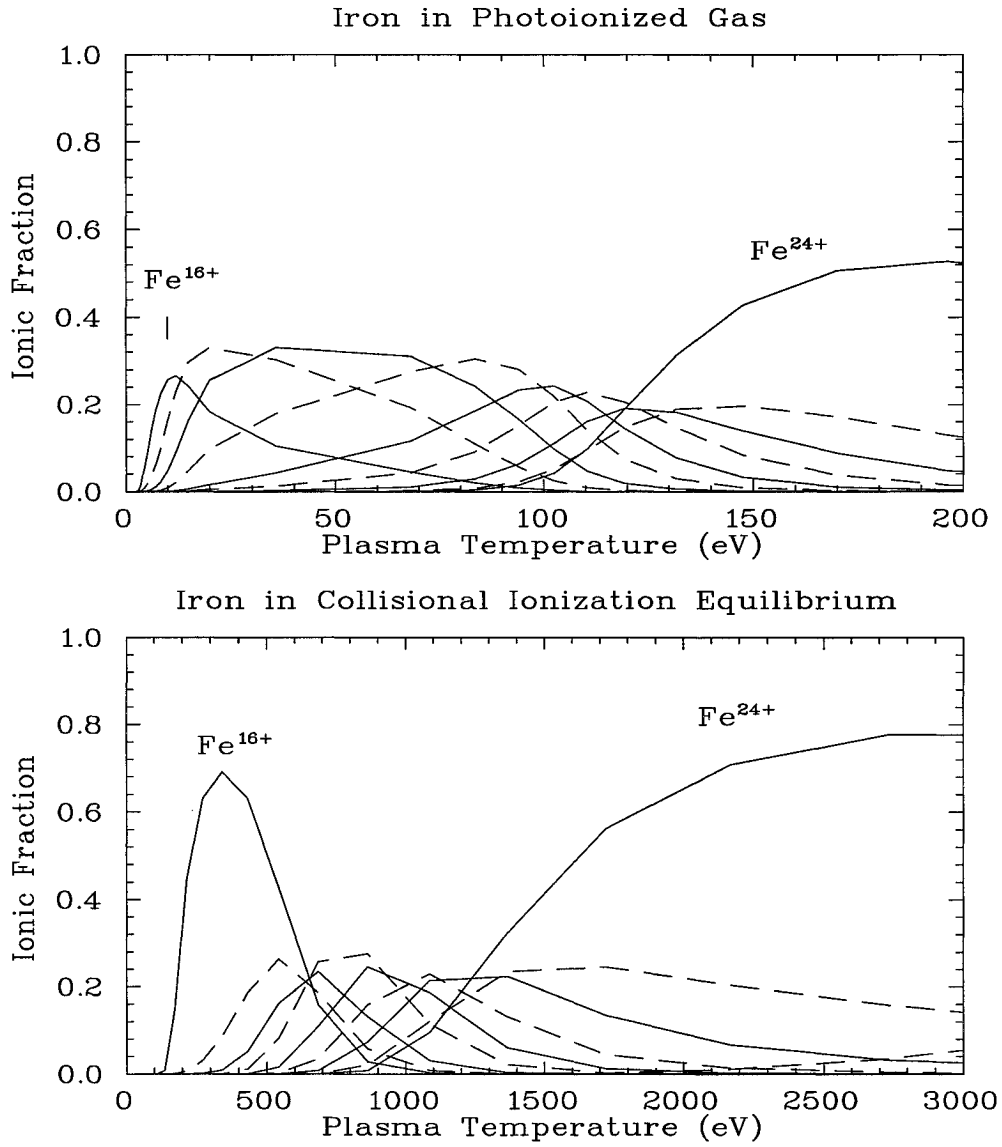

FIGURE 1. Calculated ionization equilibrium for Fe^{16+} through Fe^{24+} in a plasma with cosmic abundances photoionized by a 10 keV bremsstrahlung radiation field (top) [1] and in an electron-ionized plasma (bottom) [10].

ionization equilibrium an ion forms at an electron temperature $T_e \sim I_P/20$ (assuming cosmic abundances in the plasma), where I_P is the ionization potential of the

ion [1].

This is to be contrasted with electron-ionized plasmas which include the sun [4], stars [5], supernovae [6], and clusters of galaxies [7]. In an electron-ionized plasma the ionization structure depends, at low densities, only on the electron temperature. In ionization equilibrium an ion forms at $T_e \sim I_P/2$ [8]. Figure 1 shows the calculated ionization structure for Fe^{16+} to Fe^{24+} for both a photoionized and an electron-ionized plasma.

There is an order of magnitude difference between the temperatures at which a given ion forms in a photoionized versus an electron-ionized plasma. As a result different atomic processes are important in each plasma. In a photoionized plasma, low temperature dielectronic recombination (DR) is the dominant recombination process for most ions [9]. X-ray line emission is due primarily to radiative recombination (RR) and DR [1]. In an electron-ionized plasma, high temperature DR is the dominant recombination process for most ions [8,10]. X-ray line emission is due primarily to electron impact excitation [11,12].

Iron ions play an important role in determining the line emission and thermal and ionization structures of X-ray photoionized plasmas [1,13,14]. Of particular interest are Fe^{16+} to Fe^{23+} (L-shell iron) which affect the range in parameter space over which photoionized gas is predicted to be thermally unstable. The need to better understand this instability has been demonstrated by recent studies of the XRB Cyg X-3 which was observed by the *Advanced Satellite for Cosmology and Astrophysics*. These observations detected line emission from ions of neon, magnesium, silicon, and sulfur which are predicted to form in the region of thermal instability [2]. With the recent launches of the *Chandra X-ray Observatory* and the *X-ray Multimirror Mission* (*XMM*), many more observations are expected of line emission from ions predicted to form in thermally unstable, photoionized plasmas.

DIELECTRONIC RECOMBINATION

DR is a two-step electron-ion recombination process which begins when a free electron collisionally excites an ion, via an $nl_j \rightarrow n'l'_{j'}$ excitation of a bound core electron. Energy conservation dictates that this first step, dielectronic capture, can go forward only when the kinetic energy of the incident electron, E_k, plus the binding energy released when the electron is captured, E_b, equals the excitation energy of the core electron, ΔE. Because E_b and ΔE are both quantized, DR is a resonant process. DR is complete when the recombined ion emits a photon which reduces the total energy of the system to below its ionization limit.

The resonance structure of DR determines its T_e dependence. For L-shell iron, $\Delta \equiv n' - n = 0$ DR occurs only for $E_k \lesssim 130$ eV. $\Delta n = 1$ DR occurs only for $E_k \gtrsim 250$ eV. As a result, $\Delta n = 0$ DR is the dominant DR channel for most L-shell iron ions in photoionized plasmas and $\Delta n = 1$ DR in electron-ionized plasmas.

All of the low temperature DR rate coefficients currently used for modeling cosmic plasmas come from theoretical calculations [1,9]. However, a critical evaluation of

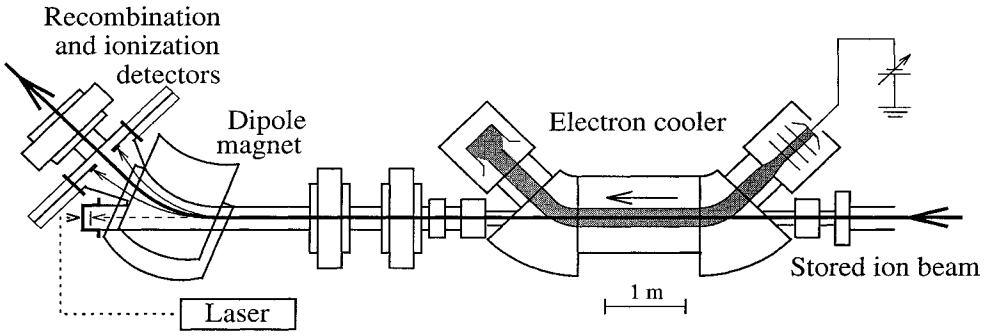

FIGURE 2. Shown is a partial overview of the TSR experimental arrangement for electron-ion collision measurements. Stored ions enter from the right. The electrons are merged with the ions and travel co-linear with them for ~ 1.5 m after which the electrons are separated from the ions. The ions then travel into a dipole magnet where recombined (ionized) ions are bent less (more) strongly than the primary beam and directed onto a particle counting detector.

published theoretical DR rates suggests a factor of 2 or more uncertainty is inherent in the different theoretical techniques used to calculate DR for ions with partially filled L or M shells [10,14,16]. This is supported by laboratory measurements which have turned up errors of factors of 2 to orders of magnitude in calculated DR rates [14,15,18,19]. The measurements also demonstrate that it is not possible *a priori* to know which set of calculations, if any, will agree with experiment. Taken all together, these results suggest that, for ions with partially filled L or M shells, a factor of ~ 2 uncertainty exists in almost all published theoretical DR rates currently used for modeling photoionized plasmas. This lack of reliable low temperature DR rates is the dominant uncertainty in the ionization balance in photoionization equilibrium [9] and translates into a corresponding uncertainty in the thermal structure and line emission of the plasma.

EXPERIMENTAL PROGRAM

To address the needs for modeling and interpreting the line emission from X-ray photoionized plasmas, we have initiated a laboratory program of low energy (i.e., low temperature) DR measurements using the heavy-ion test storage ring (TSR) at the Max Planck Institute for Nuclear Physics in Heidelberg, Germany [17]. To date, measurements have been carried out for DR onto Fe^{15+} [18] (which preceded the present program) as well as onto Fe^{17+} [14,15], Fe^{18+} [14], Fe^{19+}, Fe^{20+}, and Fe^{21+}. Evaluation is currently underway for these three latter ionization stages. Measurements of DR onto Fe^{22+} and Fe^{23+} will be carried out in the near future.

Storage rings are uniquely suited to carry out measurements of low energy DR. Commonly used techniques for measuring DR, such as electron beam ion traps [20,21] and theta pinches or tokamaks [22], can produce the desired ions but can-

not simultaneously achieve the required low energies. Crossed electron-ion beam techniques cannot achieve the desired low collision energies [23,24]. Single-pass, merged electron-ion beam techniques can achieve low collision energies, but analysis of such data, particularly for ions with partially filled shells, is usually complicated by the presence of unknown quantities of metastable ions in the ion beam [25]. Storage ring measurements are able to overcome this problem by storing the ions long enough for all the metastable levels to decay radiatively to the ground state. Storage rings can also usually run at conveniently high signal rates with low background rates.

Figure 2 shows a schematic of the portion of TSR used to perform DR experiments. Measurements are carried out by merging the ion and electron beams in one of the straight sections of TSR for ~ 1.5 m. After demerging, any recombined ions are magnetically separated from the stored ions and directed onto a detector. The relative electron-ion collision energy can be precisely controlled (from 0 to $\sim$ 2000 eV) and the recombination signal measured as a function of this energy. The experiments basically follow the procedure described in Refs. [26,27]. the accuracy of the measured DR resonance strengths is estimated to be better than 20%.

Recombination involves capturing a free electron into a Rydberg level n. Between the cooler and the dipole magnet, some of these captured electrons radiatively decay to lower-lying levels. Recombined ions where the captured electron, at the dipole magnet, is in a level $n \gtrsim n_{max}$ are field ionized by the magnet and not detected. For TSR measurements of L-shell iron, n_{max} is typically ~ 120. Calculations indicate that the contributions to the total L-shell iron, $\Delta n = 0$ DR rate coefficient from levels $n > n_{max}$ is $\lesssim 4\%$. TSR measurements of L-shell iron DR can therefore be used to produce reliable DR rate coefficients for plasma modeling. DR Rate coefficients derived from the measured DR resonance strengths are estimated to have an accuracy of better than 20%.

Experimental work has demonstrated that DR is sensitive to external electric and magnetic fields [23,24,28,29], especially crossed electric and magnetic fields [29]. However, in TSR the fields are extremely well controlled and we are able to carry out essentially field-free DR measurements. In the interaction region in TSR, external electric fields are insignificant ($E \lesssim 10$ V cm^{-1}). The ions also travel parallel to the magnetic field which confines the electrons and hence experience no $\mathbf{v} \times \mathbf{B}$ electric field. The influence on the DR measurements due to this ~ 400 G field are predicted to be negligible [30]. Additionally, $\Delta n = 0$ DR measurements on lithiumlike chlorine have shown that for DR into levels $n \lesssim 80$, electric field effects are not discernible at fields $E \lesssim 15$ V cm^{-1} [29]. Our work here involves DR measurements for ions more highly charged than lithiumlike chlorine, and the effect of external fields on the $\Delta n = 0$ DR process is predicted to decrease with increasing charge [31]. Also, theoretical calculations indicate that the contributions to the total L-shell iron, $\Delta n = 0$ DR rate coefficient from levels $n > 100$ is $\lesssim 10\%$ [14]. Therefore, we expect external fields to have an insignificant effect on the L-shell iron low temperature DR rates derived from TSR data.

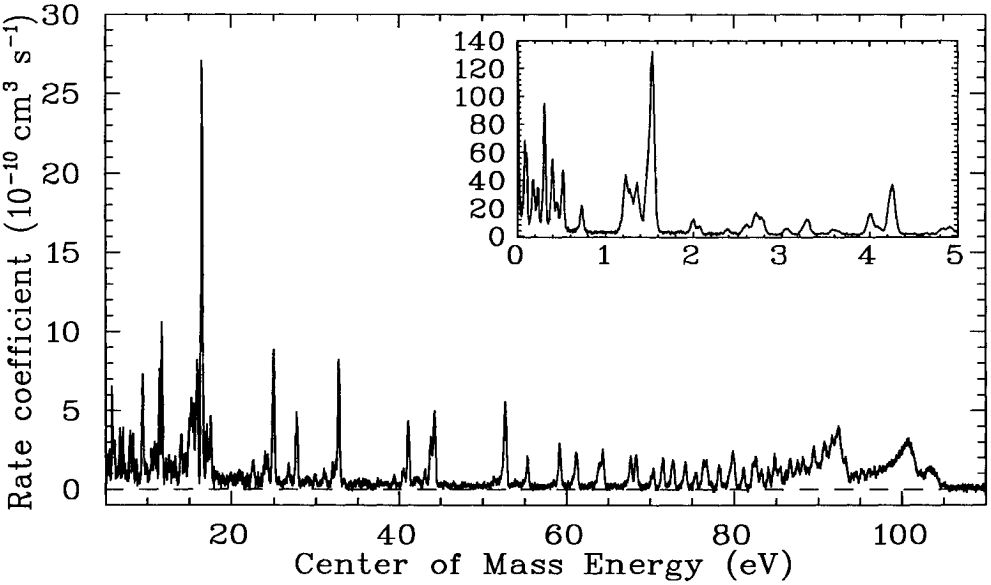

FIGURE 3. Measured Fe^{19+} to Fe^{18+} recombination rate coefficient vs. electron-ion collision energy. The data represent the convolution of the DR cross section with the energy spread of the experiment. The non-resonant "background" is due primarily to RR. Estimated systematic errors are better than ±20% for the absolute rate coefficient and ±1% for the energy scale.

RECENT RESULTS

In Figure 3 we show the data for $\Delta n = 0$ DR onto nitrogenlike Fe^{19+}. These data clearly demonstrate the resonance nature of the DR process. Following the procedures outlined in Refs. [14,26,27], we can fit the DR resonances to extract the relevant resonance strengths and energies. We then integrate the measured resonances with a Maxwellian electron velocity distribution to yield a total $\Delta n = 0$ DR rate coefficient for plasma modeling (cf., Refs. [14,15,32]).

In Figure 4 we show our experimentally-derived, Maxwellian-averaged rate coefficient for $\Delta n = 0$ DR onto Fe^{19+}. This rate coefficient does not include contributions from RR. We also show various published theoretical DR rates and the recommended RR rate. Fe^{19+} is predicted to form in a photoionized plasma of cosmic abundances at $k_B T_e \sim 80$ eV [1]. At this temperature our experimentally derived DR rate coefficient is ~ 1.3 times larger than the theoretical rates of Jacobs *et al.* (as reported in [34]) and of Roszman (as reported in [10]). However, the temperature of a photoionized plasma depends on the metallicity of the gas as well as the possible presence of additional cooling mechanisms. Fe^{19+} could thus form at cooler temperatures where the disrepancy between the experimentally derived rate and theory is significantly larger. The reason for this disrepancy is most likely due

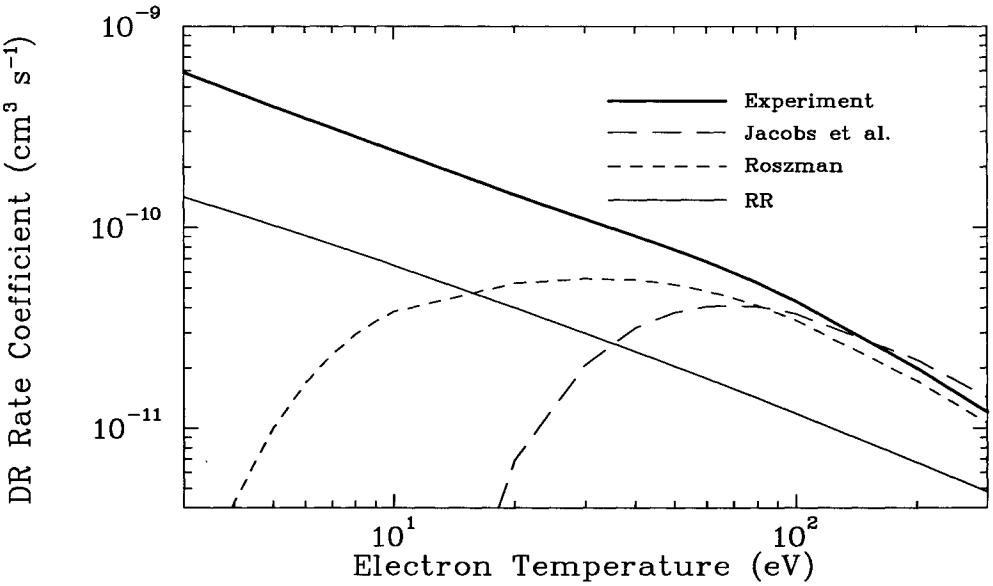

FIGURE 4. Fe^{19+} to Fe^{18+} Maxwellian-averaged $\Delta n = 0$ DR rate coefficients. The thick solid curve has been calculated using the DR data in Figure 3. The systematic error is estimated to be better than ±20%. Also shown are the $\Delta n = 0$ DR rates of Jacobs et al. [33] (long dashed curve) as fitted by Shull and van Steenberg [34] and the rates of Roszmann (short dashed curve) as reported by Arnaud and Raymond [10]. The recommended RR rate of Arnaud and Raymond [10] is the given by the thin solid curve.

to these calculations not having correctly calculated the DR resonance structure for energies below ~ 5 eV. The DR rate at $k_B T_e \sim 80$ eV is ~ 3.8 times larger than the RR rate.

We conclude this section with a warning that comparison of measured and theoretical Maxwellian rate coefficients alone cannot be used to verify the accuracy of a particular theoretical technique. Any agreement between experiment and theory may be fortuitous [14]. A detailed comparison between experimental and theoretical resonance strengths and energies is the only unambiguous way to verify the accuracy of the theoretical technique and the resulting DR rate coefficient calculations.

ASTROPHYSICAL IMPLICATIONS

There are a number of potential astrophysical implications of our work to date. For example, DR via $2p_{1/2} \rightarrow 2p_{3/2}$ core excitations offers the possibility of new electron temperature and density diagnostics [35]. Also, the estimated factor of 2 uncertainty in the published $\Delta n = 0$ DR rates for L-shell iron can dramatically

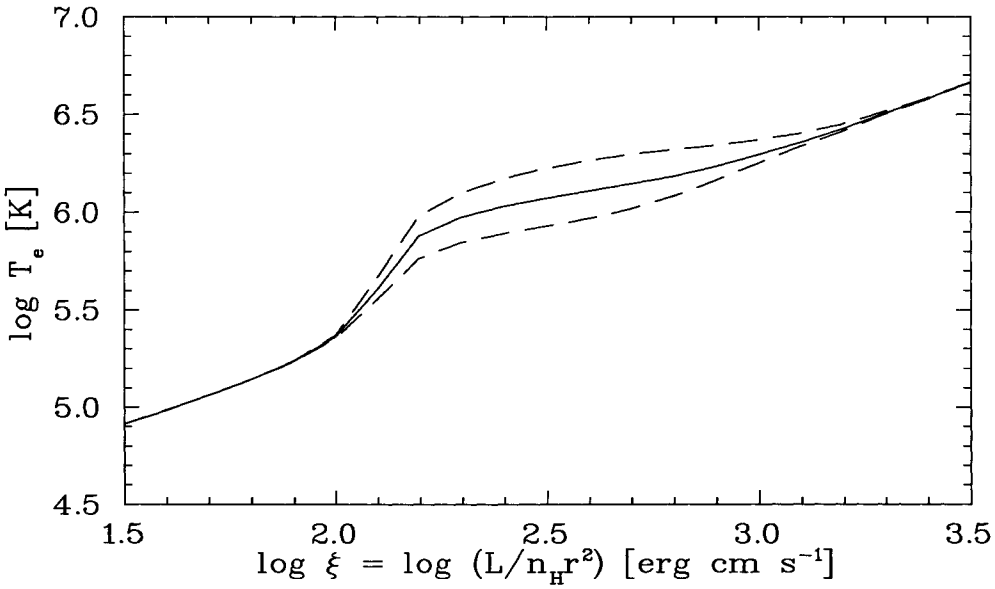

FIGURE 5. Predicted T_e versus ionization parameter ξ for a model AGN ionizing spectrum illuminating a slab of gas with cosmic abundances. The middle curve shows the predicted T_e using our experimentally derived $\Delta n = 0$ DR rates for Fe^{17+} and Fe^{18+} and the unchanged $\Delta n = 0$ DR rates for Fe^{19+} through Fe^{23+}. The upper (lower) dashed curve shows our results when the $\Delta n = 0$ DR rates for Fe^{19+} through Fe^{23+} are increased (decreased) by a factor of 2.

affect the range in parameter space over which photoionized gas is thermally unstable, making it smaller or larger. However, the uncertainty in these DR rates cannot remove the instability [14]. Here we will only discuss the implications for line emission from photoionized gas.

We have used XSTAR (version 1.40b) [36] to investigate the effects on the temperature structure and line emission of X-ray photoionized gas due to our estimated factor of 2 uncertainty in the theoretical $\Delta n = 0$ DR rates currently used for L-shell iron [14]. We have run XSTAR with the relevant $\Delta n = 0$ DR rates unchanged, increased by a factor of two, and decreased by a factor of two. We have also assumed cosmic abundances and a model AGN ionizing spectrum with a photon number power law of $N \propto E^{-1.8}$ extending from 13.6 eV to 40 keV. Here E is the photon energy.

Figure 5 shows the predicted electron temperature versus ionization parameter $\xi = L/n_H r^2$, where L is the luminosity of the ionizing source, n_H the hydrogen nucleus density, and r the distance from the ionizing source. Should a future observation yield a $\log T_e \sim 6.1$ (where T_e is in K), then the uncertainty in the inferred ξ would be a factor of ~ 3.4. For observations in this range of ξ, this uncertainty will hamper our ability to determine L or n_H to within a factor of

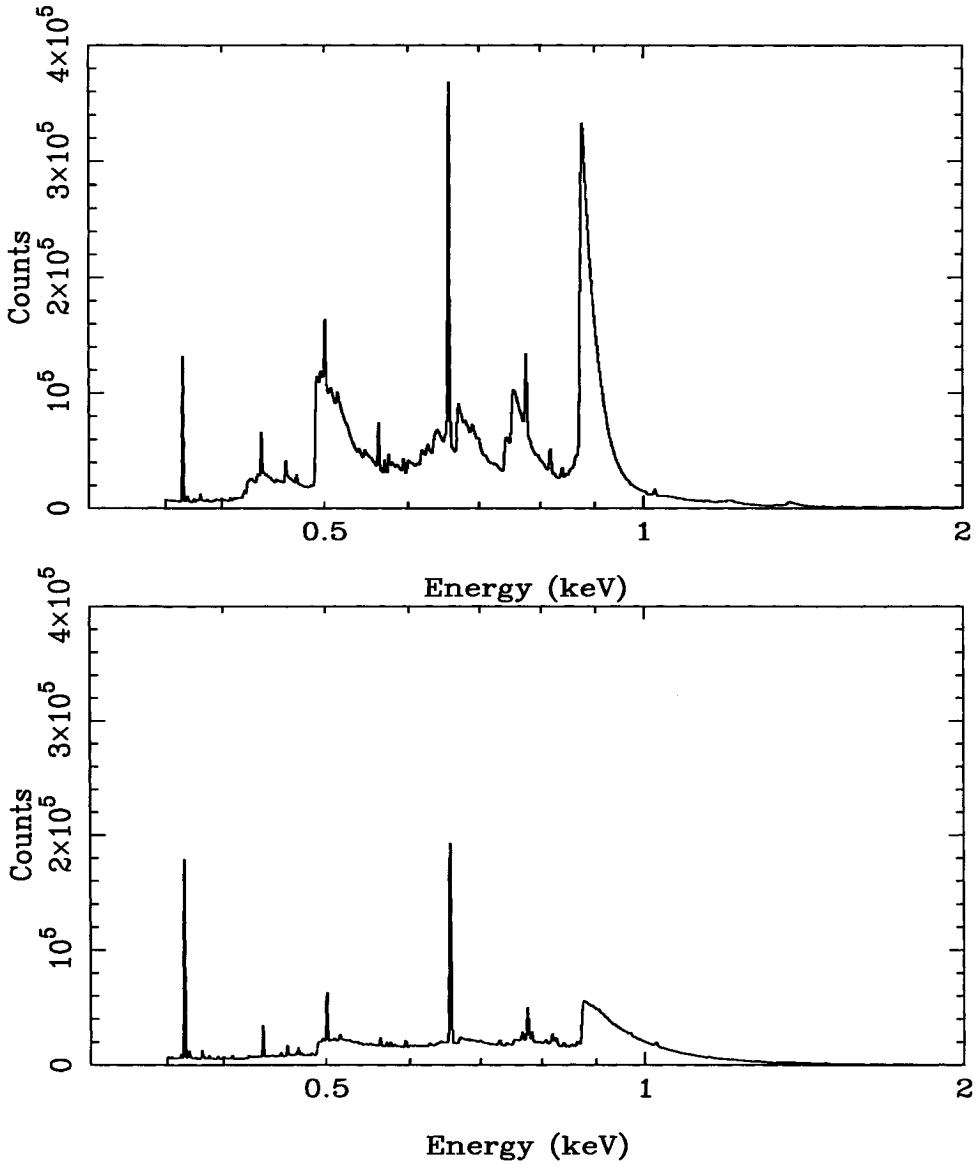

FIGURE 6. Synthetic spectra using XSTAR for a slab of photoionized gas with cosmic abundances at $\log \xi \sim 2.1$. The spectra have been folded through the *XMM*-RGS response matrix using XSPEC. We use our experimentally derived $\Delta n = 0$ DR rates for Fe^{17+} and Fe^{18+}. The Fe^{19+} through Fe^{23+} $\Delta n = 0$ DR rates have been decreased (increased) by a factor of 2 for the spectrum on the top (bottom).

~ 3.4 or r to a factor of ~ 1.8.

The estimated uncertainty in the DR rates results, for a given value of ξ, in as much as a factor of $\sim$ 1.8 variation in the predicted electron temperature. The spectroscopic implications of this temperature uncertainty are shown in Figure 6. Here we have used XSTAR to produce synthetic spectra which we have folded through the *XMM* Reflection Grating Spectrometer (RGS) using XSPEC [37]. The dramatic difference between the two spectra in Figure 6 is due to the different temperatures for the two test cases. The temperature dramatically affects the width of the radiative recombination continua seen in the spectra and in the line-to-continuum ratios.

ACKNOWLEDGEMENTS

We thank the staff and technicians of the TSR group for support during the beam time. We also thank A. Rasmussen for providing the *XMM*-RGS response matrix for the synthetic spectra. This work was supported in part by NASA High Energy Astrophysics X-Ray Astronomy Research and Analysis grant NAG5-5123 and NASA Space Astrophysics Research and Analysis grant NAG5-5261. Travel and living expenses for DWS were supported by NATO Collaborative Research Grant CRG-950911. The experimental work has been supported in part by the German Federal Minister for Education, Science, Research, and Technology (BMBF) under Contract Nos. 06 GI 475, 06 GI 848, and 06 HD 854I. Work performed at Lawrence Livermore National Laboratory was under the auspices of the US Department of Energy (contract number W-7405-ENG-48).

REFERENCES

1. Kallman, T. R., Liedahl, D. A., Osterheld, A., Goldstein, W., and Kahn, S., *Astrophys. J.* **465**, 994 (1996).
2. Liedahl, D. A., and Paerels, F., *Astrophys. J. Lett.* **468**, L33 (1996).
3. Nandra, K., George, I. M., Mushotzky, R. F., Turner, T. J., and Yaqoob, T., *Astrophys. J.* **477**, 602 (1997).
4. Doschek, G. A., and Cowan, R. D., *Astrophys. J. Suppl. Ser.* **56**, 67 (1984).
5. Mewe, R., *Astron. Astrophys. Rev.* **3**, 127 (1991).
6. Hwang, U., and Gotthelf, E. V., *Astrophys. J.* **475**, 665 (1997).
7. Fabian, A. C., Arnaud, K. A., Bautz, M. W., and Tawara, Y., *Astrophys. J. Lett.* **436**, L63 (1994).
8. Mazzotta, P., Mazzitelli, G., Colafrancesco, S., and Vittorio, N., *Astron. Astrophys. Suppl. Ser.* **133**, 403, (1998).
9. Ferland, G. J., Korista, K. T., Verner, D. A., Ferguson, J. W., Kingdon, J. B., and Verner, E. M., *Publ. Astron. Soc. Pacific* **110**, 761 (1998).
10. Arnaud, M., and Raymond, J., *Astrophys. J.* **398**, 394 (1992).
11. Raymond, J. C., and Smith, B. W., *Astrophys. J. Suppl. Ser.* **35**, 419 (1977).

12. Mewe, R., Gronenschild, E. H. B. M., and van den Oord, G. H. J., *Astron. Astrophys. Suppl. Ser.* **62**, 197 (1985).
13. Hess, C. J., Kahn, S. M., and Paerels. F., *Astrophys. J.* **478**, 94 (1997).
14. Savin, D. W., Kahn, S. M., Linkemann, J., Saghiri, A. A., Schmitt, M., Grieser, M., Repnow, R., Schwalm, D., Wolf, A., Bartsch, T., Brandau, C., Hoffknecht, A., Müller, A., Schippers, S., Chen, M. H., and Badnell, N. R., *Astrophys. J. Suppl. Ser.* **123**, 687 (1999).
15. Savin, D. W., Bartsch, T., Chen, M. H., Kahn, S. M., Liedahl, D. A., Linkemann, J., Müller, A., Schippers, S., Schmitt, M., Schwalm, D., and Wolf, A., *Astrophys. J. Lett.* **489**, L118 (1997).
16. Savin, D. W., *Astrophys. J.* **553**, 106 (2000).
17. Müller, A., and Wolf, A., in *Accelerator-Based Atomic Physics Techniques and Applications*, ed. S. M. Shafroth, and J. C. Austin, New York: American Institute of Physics, 1997, p. 147.
18. Linkemann, J., Kenntner, J., Müller, A., Wolf, A., Habs, D., Schwalm, D., Spies, W., Uwira, O., Frank, A., Liedtke, A., Hofman, G., Salzborn, E., Badnell, N. R., and Pindzola, M. S., *Nucl. Instrum. Methods* **B98**, 154 (1995).
19. Schippers, S., Bartsch, T., Brandau, C., Gwinner, G., Linkemann, J., Müller, A., Saghiri, A. A., and Wolf, A., *J. Phys. B* **31**, 4873 (1998).
20. Beiersdorfer, P., Brown, G. V., Crespo López-Urrutia, Decaux, V., Elliot, S. R., Savin, D. W., Smith, A. J., Stefanelli, G. S., Widmann, K., and Wong, K. L., *Hyperfine Interactions* **99**, 203 (1996).
21. Gu, M. F., Kahn, S. M., Savin, D. W., Beiersdorfer, P., Brown, G. V., Liedahl, D. A., Reed, K. J., Bhalla, C. P., and Grabbe, S. R., *Astrophys. J.* **518**, 1002 (1999).
22. Griem, H. R., *J. Quant. Spectrosc. Radiat. Transfer* **40**, 403 (1988).
23. Müller, A., Belić, D. S., DePaola, B. D., Djurić, N., Dunn, G. H., Mueller, D. W., and Timmer, C., *Phys. Rev. A* **36**, 599 (1987).
24. Savin, D. W., Gardner, L. D., Reisenfeld, D. B., Young, A. R., and Kohl, J. L., *Phys. Rev. A* **53**, 280 (1996).
25. Badnell, N. R., Pindzola, M. S., Anderson, L. H., Bolko, J., and Schmidt, H. T., *J. Phys. B* **24**, 4441 (1991).
26. Kilgus, G., Habs, D., Schwalm, D., Wolf, A, Badnell, N. R., and Müller, A., *Phys. Rev. A* **46**, 5730 (1992).
27. Lampert, A., Wolf, A., Habs, D., Kilgus, G., Schwalm, D., Pindzola, M. S., and Badnell, N. S., *Phys. Rev. A* **53**, 1413 (1996).
28. Bartsch, T., Müller, A., Spies, W., Linkemann, J., Danared, H., DeWitt, D. R., Gao, H., Zong, W., Schuch, R., Wolf, A., Dunn, G. H., Pindzola, M. S., and Griffin, D. C., *Phys. Rev. Lett.* **79**, 2233 (1997).
29. Bartsch, T., Schippers, S., Müller, A., Brandau, C., Gwinner, G., Saghiri, A. A., Beutelspacher, M., Grieser, M., Schwalm, D., Wolf, A., Danared, H., and Dunn, G. H., *Phys. Rev. Lett.* **82**, 3779 (1999).
30. Huber, W. A., and Bottcher, C., *J. Phys. B* **13**, L399 (1980).
31. Griffin, D. C., and Pindzola, M. S., 1987, *Phys. Rev. A* **35**, 2821 (1987).
32. Savin, D. W., *Astrophys. J.* **523**, 855 (1999).
33. Jacobs, V. L., Davis, J., Kepple, P. C., and Blaha, M., *Astrophys. J.* **211**, 605 (1977).

34. Shull, J. M., and van Steenberg, M., *Astrophys. J. Suppl. Ser.* **48**, 95 (1982); Erratum **49**, 351 (1982).
35. Savin, D. W., Bartsch, T., Chen, M. H., Kahn, S. M., Liedahl, D. A., Linkemann, J., Müller, A., Schippers, S., Schmitt, M., Schwalm, D., and Wolf, A., in *NIST Special Publication 926, Poster Papers, International Conference on Atomic and Molecular Data and Their Applications (ICAMDATA 97)*, ed. W. L. Wiese and P. J. Mohr, Washington, D.C.: U.S. Government Printing Office, 1998, p. 96.
36. Kallman, T. R., and Krolik, J. H., *XSTAR, A Spectral Analysis Tool* (1997); available at http://heasarc.gsfc.nasa.gov/docs/software/xstar/xstar.html.
37. Arnaud, K, and Dorman, B., *Xspec, An X-Ray Spectral Fitting Package* (2000); available at http://legacy.gsfc.nasa.gov/docs/xanadu/xspec/index.html.